Benchmarking Resilience of Artificial Hands

F. Negrello[1], M. Garabini[2], G. Grioli[1], N. Tsagarakis[1], A. Bicchi[1,2] and M. G. Catalano[1]

***Abstract*— The deployment of robotics in real-world scenarios, which may involve harsh and irregular physical interactions with the environment, such as those when robots operating in a disaster scenario, or the interactions that prosthetic devices may experience, demands hardware, which is physically resilient. The end-effectors, as the main media of interaction, are probably the parts at the highest risk. The capability of robotic hands to survive severe impacts is thus a necessity for the effective deployment of reliable robotic solutions in real-world tasks. Although, this robustness capability has been noted and discussed in the robotics community for long time, the literature does not provide a systematic study nor there is any proposal of standardized test or metric to evaluate hand resilience. In this work, inspired by the works of Charpy and Izod for the systematic definition of resilience and toughness of materials through impact tests, we consider extending the standard test to robot hands. We introduce a resilience evaluation framework, including a precisely defined experimental set-up and test procedure. As an example of application of the procedure, we apply it to experimentally characterize two robot hands, with a similar conceptual architecture but different size and material. From these tests we obtain several insights, including the observation that the dominant factor in hand resilience is their compliance and actuation principle, and that the use, under certain design conditions, of lightweight materials, such as plastic instead of aluminum, may not necessarily reduce the mechanical strength of the overall system.**

I. Introduction

Robots are facing a rapidly expanding range of potential applications beyond the lab, from remote exploration [1] and search-and-rescue [2] to agriculture [3], household assistance [4] and prosthetics [5]. In real-world activities, the focus of interaction is often via the robotics end-effectors, which experience severe conditions. Consequently, the robotic hand/gripper capability to withstand sporadic (but not infrequent) high energy impacts, i.e. sport activities in Fig. 1, is an essential requirement. In this regard, we address the characterization of robotic end-effectors robustness to impulsive loads. The relevance of the problem of robotic hands robustness was firstly identified and popularized by Grebenstein, who used to motivate some aspects of the design of DLR hand fingers [6], by slamming his fingers on the edge of the podium and stating that one important, although often disregarded, design goal was to make a robot capable of withstand that. In the field some started to refer to this as "Grebenstein test". However, the problem of the robustness of robotic hands has been discussed in literature only through anecdotal demonstrations, such as dropping an end-effector from a certain height or forcing it to collide at a known speed on an obstacle or hammering it (Fig. 2). Commonly, the term *resilience* is used as synonym of robustness for a part or a material that can withstand with high loads without fracturing. That's because material resilience in engineering represents its capability of absorbing energy elastically. Considering robot hands, it is important to evaluate both the impact energy they can withstand and the loads they transfer to the structure, which in robots may cause damage to other components (e.g. actuators, F/T sensors), while in prosthetic applications, affects the user's comfort. On this base, we propose a test complementary to the NIST's tests for benchmarking robotic hands grasping [7]. We focused on assessing their mechanical resilience (hereinafter resilience) and represents a preliminary investigation on a novel set of parameters for characterizing and comparing robotics systems, independently from their specific implementation and control framework. Our approach is based on the Charpy and Izod impact test, which are methods to characterize materials toughness. We propose *joint mobility* as the possibility of dislocating the hand's joints without damages, which provides a static description of the hand structure. While *energy absorbed* and *forces transmitted* through its structure are used to define the dynamics of the system. To fully characterize a robotic hand it is important to consider all the parameters: whether the system is stiff or soft, where the impact happens, how large the impact area is (i.e. one finger in contact or more), and on which direction the hand is loaded.

Fig. 1. Photo-sequence of a prosthetic user executing a float service.

This project has received funding from the European Union's Horizon 2020 research and innovation programme under grant agreement SOFTPRO (no. 688857), SOMA (no.645599) and ILIAD (no.732737). The content of this publication is the sole responsibility of the authors. The European Commission or its services cannot be held responsible for any use that may be made of the information it contains.

[1] Istituto Italiano di Tecnologia, Via Morego 30, 16163, Italy, e-mail: francesca.negrello@iit.it.

[2]Centro di Ricerca "Enrico Piaggio" e Dipartimento di Ingegneria dell'Informazione, University of Pisa, Largo Lucio Lazzarino 1, 56126 Pisa, Italy.

More than 500 impact tests have been done, considering stiff and compliant hand configurations, different number of fingers and of phalanxes in contact (impact conditions), and different pendulum masses (load levels). Experimental tests prove that the energy absorbed by a compliant hand depends on its stiffness (related to the portion of the hand in contact) and not on the actual load level. The energy absorbed, and consequently the transmitted loads, result strongly reduced when compared to an equivalent stiff case. In this regards, soft robotic hands, which in their widest connotation include soft continuous robots [8] [9], variable stiffness [10] and under-actuated hands [11] [12], are capable of deforming elastically, reducing the loads transmitted and consequently preventing structural damage due to shocks [6]. Moreover, we demonstrated that if robustness is enhanced by design (soft robotic design), the use of lightweight materials, such as plastic, is possible without sacrificing the mechanical strength of the overall system. This work experimentally demonstrated that the ideas presented are a viable solution for evaluating the soft robotic hands resilience. The authors did not intended to present a definitive methodology, hoping instead that this work represents a first draft on which base extend the discussion to the robotic community.

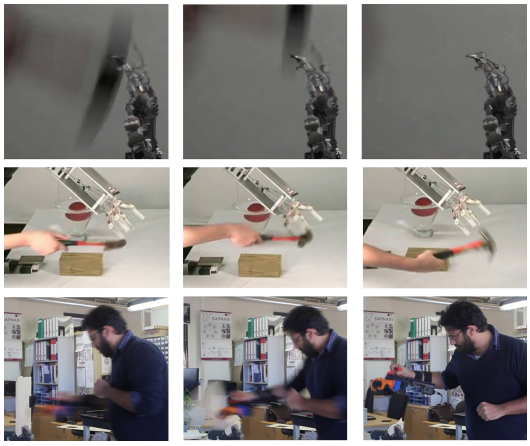

Fig. 2. Photo-sequence of the robotic hands during impact test in lab, from top to bottom the DLR David's hand [13] [10], the SDM hand [14] [11] and the Pisa-IIT SoftHand [12].

II. From Standard Specimens to Robotic Hands

In material science and engineering, the capability of absorbing energy through material deformation is described by toughness, resilience and ductility. As in Fig. 3(a), toughness is the ability of a material to absorb energy through plastic deformation without fracturing, resilience is the material capability to store elastic energy, whereas ductility is the ability to plastically deform under tensile stress [15]. Izod and Charpy impact test are the standards for quantifying the material toughness both for metals and plastics. The test consists in loading with an impulsive force a notched specimen causing its fracture. The material's notch toughness is evaluated measuring the energy absorbed during fracture. The main difference between the two tests is the orientation

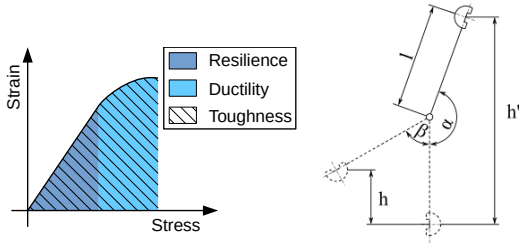

(a) (b)

Charpy Classification	
low	<30J
medium	30J - 110J
high	110J - 200J
ultra-high	≥200J

(c)

Izod Classification	
Plastic	<21.7J
Tempered steel	<136J

(d)

Fig. 3. Izod impact test definitions. (a) shows the diagram which describes the principal material mechanical properties such as resilience, toughness and ductility. (b) reports the Izod pendulum scheme and the principal test parameters. (c-d) report respectively the absorbed energy levels in the Charpy and Izod impact standards.

of the specimen with respect to the pendulum. In the Charpy test the specimen is loaded as a simply supported beam, while in the Izod one it is loaded as cantilever beam. For our consideration we refer to the Izod test which is closer to the finger load condition [16] [17]. The testing machine is a pendulum with a fixed mass and length, see Fig. 3(b). During the test, the pendulum is raised at a known height (h') and released. On the vertical line the pendulum impacts on the test piece, which should be fractured by a single blow. The pendulum position is recorded during the experiment. The absorbed energy (W) is evaluated comparing the different height of the hammer before and after the fracture. The standards define a minimum number of 5 test pieces and materials classification is based on absorbed energy, as in Fig. 3(c). Note that, W shall not exceed the 80% of E_0, and it is assumed the velocity of the pendulum is constant, otherwise the accuracy of the measurement is reduced [18]. Compared to Izod standardized specimens, a robotic hand is characterized by a multiplicity of design features and components, that affect its behavior during impacts. The main components are: the structure, intended as the main support frame to which are connected all the hands kinematic chains (fingers etc.); the link frames (phalanxes); the joints, which determine the connection between phalanxes; the actuators, which provide motion to the hand, and finally the transmission which is the link between the actuation sources and the phalanxes. Depending on the actuation and transmission arrangements, part of the absorbed energy can be dissipated internally to the hand without causing damage. Therefore, it is important to identify the portion of the external load that is effectively transmitted to the structure, through the actuation. Although theoretically possible, the analytical evaluation of the hand dynamics is not a viable option for benchmarking purposes, due to the large variety of implementations and the difficulty of extracting all the

parameters. In the multimedia material we report the analysis of simplified models to provide a general understanding of the dynamic behavior of different state of art hand designs.

III. Proposed Approach

We present the proposed metrics and methodology for experimentally characterize robotic hands resilience, independently from their physical implementation.

1) Metrics: Hands dynamics can be described by local and global properties. A relevant local parameter is the capability of the joint itself of being dislocated (taken apart) without structural damage, both in the plane of the joint axis and perpendicularly to it, as in Fig. 5. Thus, we define joint mobility as the maximum passive displacement allowed between two phalanxes. It can be either rotational or linear (Fig. 5(a)-5(f)) and should be evaluated along the main hand planes, as in Fig. 4. To evaluate the global characteristics of soft robotic hands in highly dynamic interactions, we borrowed the concepts from the Izod impact test. Similarly, it is possible to evaluate the energy absorbed (W) by the hand during impacts. W is the energy required to deform a hand or part of it, when a contact happens. Note that soft robotic hands resilience, is due to elastic deformations. Therefore, the hand resilience is inversely proportional to W. A high value of W means that a high portion of impact energy is transferred to the system. Another parameter is the load transmission. As matter of fact, the loads generated during impacts travel along the structure, whereas a deformation occurs, part of the energy is dissipated generating consequently a reduction of the transmitted loads. Intuitively, hand resilience quantifies the portion of the energy absorbed by the system from the impact with the environment (pendulum), while the force quantifies the energy dissipated within the hand deformation. Consequently, the higher is the hand resilience, the lower are the loads transmitted to its structure and to its base (wrist).

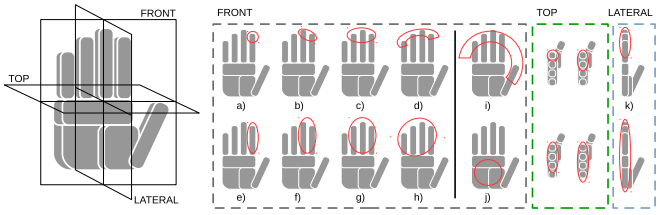

Fig. 4. Picture (a) shows the hands reference planes and the different impact regions on each plane. The letters identify the experimentally tested cases: a) single finger, distal phalanx; b) two fingers, distal p.; c) three fingers, distal p.; d) four fingers, distal p.; e) one finger, full; f) two fingers, full; g) three fingers, full; h) four, full; i) five fingers full; j) palm, k) lateral impact on the fingers.

Summarizing, the proposed parameters are:

- **Joint mobility:** as the capability of dislocating elastically the hand's joints from their axis, measured in degrees (rotational motion) or mm (linear motion).
- **Absorbed Energy:** as the capability of elastically deform during impacts reducing thus the severity of the loads (J).

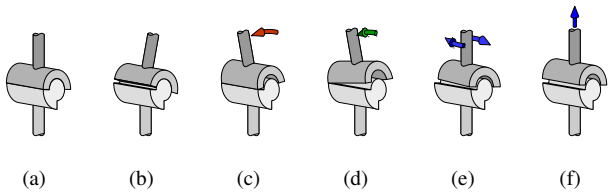

Fig. 5. Examples of joint mobility in the different planes are reported: the undeformed finger joint (b), the joint partially bend (c), a backward bend (d), a side bend (e), a twist (f) and a longitudinal dislocation (g).

- **Transmitted Force:** as the peak force measured at the wrist during the impact (N).

These allow for a comparison between different state of art soft robotic hand or gripper designs, eventually their application can be extended to hands with conventional joints or grippers based on different principles, i.e. jamming effect grippers [19].

2) Methodology: the effects of external loads depend on the hand configuration and on the portion of the hand involved (see technical Annex Sec. I). Considering anthropomorphic hands, we can define three principal planes: front, lateral and top, as in Fig. 4. Depending on the load direction, the finger joints can be selectively compliant [20] or in singular configurations, e.g. loads perpendicular to the top plane, therefore, the hand resilience should be evaluated under loads in different planes. Moreover, considering impacts in the front plane, it is possible to have different contact conditions, depending if one or more fingers, or a different number of phalanxes, are in contact with the environment. Consequently, to fully characterize a soft robotic hand, impact tests on the three principal planes should be considered. **Front plane:** Fig. 4 shows the different impact conditions in the front plane, from 1 to 5 fingers and one or more phalanxes in contact. Impact conditions from *(a)* to *(d)* and *(e)* to *(h)* (Fig. 4) increasing the number of fingers in contact with the striker become progressively more severe due to an incremental system stiffening. In the discussion of the results we refer to cases *(a)* to *(d)* as distal phalanx, which is where the contact happen, while cases *(e)* to *(h)*, which interest the full finger, are named proximal phalanx. Case *(i)* represents the condition in which all the five fingers get in contact with the striker. The impact condition *(j)* can be considered a reference case of impacts occurring on a completely rigid hand-wrist system. **Top plane:** the number of fingers in contact should be evaluated (Fig. 4), while it is not possible to variate the number of phalanxes. **Lateral plane:** as shown in Fig. 4 impacts will affect either the full four fingers *(k)*, thumb excluded, or the palm. The latter is equivalent to a rigid case, such as *(j)* in the front plane. Front and lateral impacts can be performed with a pendulum-like set-up, which provides repeatable impulsive loads on the hand. Each experiment is executed as follows: the pendulum falls down from a fixed position and impacts the hand that is placed close to the vertical position of the pendulum, in order to perform the specific impact condition depicted in Fig. 4. To realize impact condition with different severity

(high-medium-low energy) the tuning of the pendulum mass and/or its starting position (θ_0) should be allowed. During the experiment the hand is actively controlled to keep its rest posture. Note that impacts along the top plane normal allow to characterize the hand with the fingers in a singular configuration. Therefore, it is not possible to employ a pendulum structure to perform impacts in the top plane. A different set-up should be realized, one option is to impose a known linear displacement to the fingers. Any other impact case in the top plane, which does not consider the fingers in singularity, e.g. on a hand partially closed, is attributable to the frontal plane case. For this reason we focused our experimental activity on front and lateral plane, considering as future development the extension to top impacts for the specific case of singular fingers configuration.

IV. Impact Tests Set-up

To easy the accessibility and diffusion of the proposed testing method, we realized a custom designed system, developed with standard easy to reach components and the design will be open sourced through the Natural Machine Motion Initiative [21]. The system consist of a mechanical pendulum with a fixed length (Fig. 6). A mass is attached on the free end of the pendulum. Its oscillations are measured by a magnetic encoder (Austrian Microsystem AS5045). The hand is fixed to the base of the mechanical frame and it is connected to a Force/Torque Sensor (ATI OMEGA 160). Therefore, it is possible to evaluate the energy absorbed during the impact through the measure of the pendulum angular position, like in the Izod test (Fig. 3(b)) and the transmitted loads. The pendulum can impact the hand in

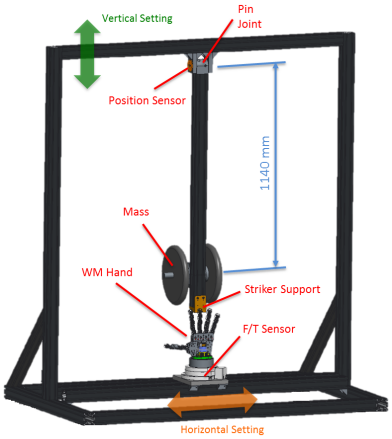

Fig. 6. Experimental set-up, the arrows (green and orange) represent the possible setting movements.

different positions (single phalanx or multiple phalanxes, single finger or multiple fingers) with several kind of strikers, that can be arranged for each specific impact experiment. The set-up allows also, to tune the mass and the starting position of the pendulum to perform impacts with different energy levels. Tab. I reports the testing conditions and pendulum configuration of each load level tested, e.g. mass, starting position, linear velocity at the impact (V_{imp}), pendulum momentum and its energy. According to Fig. 3(c), it is possible to identify the severity of the impact as low, medium and high, based on the pendulum initial energy. In the following, the load level will be indicated with the reference letter as in Tab. I. Experiments were performed on two soft robotic hands developed by our group: the WALK-MAN Hand [2] and the Pisa/IIT SoftHand [12]. In the following those will be named WM and SH respectively.

TABLE I

Testing conditions and pendulum configuration for each load level, low medium and high energy.

	Load Level	Mass (kg)	θ_0 (deg.)	V_{imp} (m/s)	Momentum (kg m/s)	E_0 (J)
Low	A_{20}	4.8	20°	1.2	5.6	3
	A_{30}	4.8	30°	1.7	8.3	8
	A_{40}	4.8	40°	2.3	11.0	12
	A_{45}	4.8	45°	2.6	12.3	16
	A_{50}	4.8	50°	2.8	13.6	19
	B_{35}	6.8	35°	2	9.6	9.7
Medium	A	4.8	90°	4.7	22.7	54
	B	6.8	90°	4.7	32.2	76
	C	7.8	90°	4.7	36.9	87
	D	8.8	90°	4.7	41.6	98
High	E	16.8	90°	4.7	79.4	188
	F	26.8	90°	4.7	126.7	300

TABLE II

Experiment table overview with reference to Fig. 4. The experiments performed only on WM are labeled with □, SH ones by △, while ○ identifies those executed on both the hands. The sign ⊘ labels those configurations excluded due to the reaching of the maximum allowed loads on the F/T sensor, ◇ labels non-significant configurations.

Load Level	Dist. Phal. a	b	c	d	Prox. Phal. e	f	g	h	Full i	Palm j	Lat. k
A_{20}	◇	◇	◇	◇	◇	◇	◇	◇	○	◇	◇
A_{30}	◇	◇	◇	◇	◇	◇	◇	◇	○	◇	◇
A_{45}	○	○	○	○	○	○	○	○	◇	◇	◇
A_{50}	◇	◇	◇	◇	◇	◇	◇	◇	◇	△	◇
B_{35}	◇	◇	◇	◇	◇	◇	◇	◇	◇	□	◇
A	○	○	○	○	○	○	○	○	⊘	⊘	○
B	○	○	○	○	○	○	○	○	⊘	⊘	△
C	△	△	△	△	△	△	△	△	⊘	⊘	△
D	△	△	△	△	△	△	△	△	⊘	⊘	△
E	□	□	□	○	□	□	□	○	⊘	⊘	△
F	□	□	□	○	□	□	□	○	⊘	⊘	△

V. Experimental Results

Tab. II summarizes the different experiments done for each load level and for any impact case. We used different symbols to identify the different experiments. Our study spanned different energy levels (low-medium-high). The lower boundary was determined by the definition of impulsive load test. Hand compliance increases the contact duration, with a consequent peak force reduction. Therefore, energy levels with low impact velocity, do not satisfy the condition of impulsive load, although, were necessary for impact conditions implying high loads on the system, such as (i) and (j). Most of the results regard medium-high energy levels. Over a certain initial energy, instead, the pendulum height variation due to the impact is small, e.g. in Fig. 7(a) where the curves of load levels E and F result almost superimposed, causing a saturation like effect, which determines the the upper boundary. The load levels for the impact test on each hand

have been selected depending on the hands characteristics (phalanx mass and joint compliance). WM was tested on the full scale of pendulum energies: high (E-F) medium (A-B) and low (A_{45}), while SH was tested on medium (A-B-C-D) and low (A_{45}). SH has been tested with (E-F)-impact case (d) and (h) to prove its capability to survive high energy/momentum impacts. Impact test have been performed in the front and lateral plane. For each impact condition and load level, five repetition have been done, with the exception of the (j) case (palm) which is reported as a reference value for stiff case. In (j), despite lowering the initial pendulum energy, the force measurement was close to the F/T sensor saturation, therefore no repetitions were performed to preserve the hardware of the experimental apparatus. Moreover, it was required to diversify the load level, B_{35} for WM and A_{50} for SH, in order to avoid to damage the load cell.

*1) **Absorbed energy**:* Fig. 7 shows phase plots of the pendulum position for the two hands, WM left column, SH right column. θ and $\dot{\theta}$ are respectively the adimensional values of the pendulum position and velocity. The top graphs compare different load levels over impact condition (g) (3 fingers-prox. phalanx), while the bottom ones compare different impact cases (e-h) over load level A. The pendulum height variation (W) depends both on its energetic level (Fig. 7 a-b) and on the number of fingers in contact (Fig. 7 c-d). It is worth noticing that, increasing the **pendulum energy**, the difference among the impact conditions become less relevant causing the saturation-like effect, see 3E-3F curves in Fig. 7(a). Increasing the **number of fingers** in contact during the impact corresponds to a hand stiffening, therefore W increases, the same trend is visible increasing the **number of phalanxes** in contact (Tabs. III(a) and III(b)). In the multimedia material we report the graphs for all the tested conditions. For a quantitative analysis, Tabs. III(a) and III(b) report the average, over the repetitions, of the energy absorbed for all the impact conditions except (i), which is reported in Tab. III(c). For all the cases we reported the percentage of *W* and not the absolute value in (J). The impact over the full hand (condition *i*), it is the most severe after the stiff case. In this case the pendulum cannot completely deform the hand and bounces back. Consequently, the values reported in Tab. III(c) approximate the stiff case. Note that Tab. III(c) reports the percentage of the absorbed energy over the five repetitions. As already stated, the condition of impulsive loads is respected for very compliant configurations (1-2 fingers in contact) or for medium-high energy (A-F), being W during the impact below 30%, while for low impact velocity the interaction forces are close to static contacts (W $\sim$ 80%). Increasing the number of fingers, W grows becoming progressively comparable with impacts on a rigid system. To characterize the system, free runs of the pendulum were executed for the different load levels. These tests revealed that energy dissipation, due to friction on the pendulum bearings, is below 1%.

*2) **Transmitted Force**:* Figs. 8(a) and 8(b) report respectively the results of impacts case a-d in the frontal plane

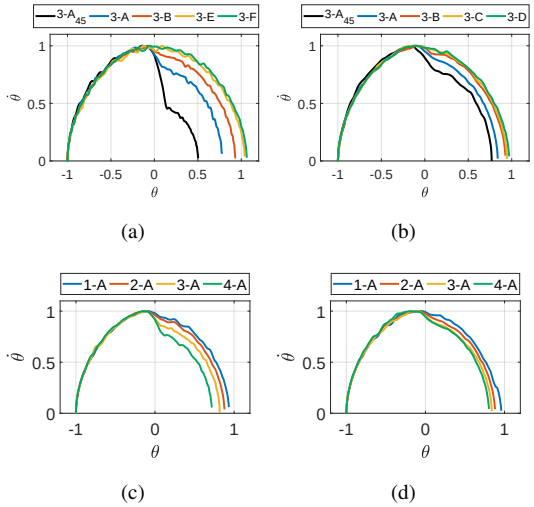

Fig. 7. Figure compares pendulum phase plot for WM (left) and SH (right). a) and b) compare all the load cases over the same impact condition (g). c) and d) compare different impact condition over the same load level.

for WM and SH. The bars show the median of the load peaks, while the whiskers report the maximum and minimum of load peaks among the impacts repetitions. The impact on the palm (impact condition *j*) is reported as reference for the impact load on a rigid system (load level A_{50} and B_{35}). It is important to highlight that under the stiff impact condition (*j*) the F/T calibration limits have been reached, which represent a technological limit of the presented set-up. Note that, the forces transmitted through the fingers are smaller compared to the stiff case. Experiments demonstrated that, when the collision happens on under-actuated compliant hands, the loads transferred at the wrist, are sensibly reduced. Generally, the trend of the forces confirms the considerations already stated for the absorbed energy, increasing the number of fingers (or phalanxes) in contact produces progressively higher loads, whereas the variation produced by different load levels are less relevant.

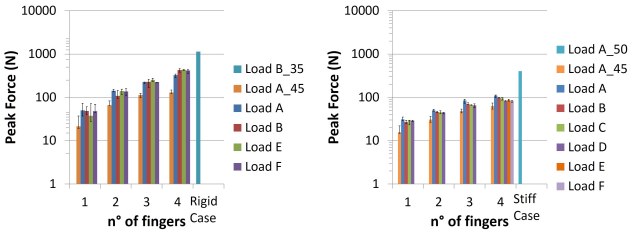

Fig. 8. Figure shows the peak forces measured during impact test a-d/all load level respectively on a) WM, b) SH, and c) SH impact case k all load level. Bars show the median value of each experiment, while the box-plot represents the statistical deviation given by the experimental measurements. For the stiff condition (j) it is reported just the value of the single trial.

VI. Discussion and Corollary Findings

We conducted more than 250 impacts on each hand on the front and lateral plane, testing the hands over 12 different

TABLE III

PERCENTAGE (%) OF ABSORBED ENERGY FOR EACH HAND (A-B). TAB. (C) REPORTS THE ENERGY ABSORBED FOR THE 5 FINGERS IMPACTS (CASE *i*). VALUES ARE EXPRESSED AS PERCENTAGE OF THE PENDULUM INITIAL ENERGY FOR EACH LOAD LEVEL AND IMPACT CASE.

(a)

WM	**Dist. Phal.**				**Prox. Phal.**				**Palm**
Load	*a*	*b*	*c*	*d*	*e*	*f*	*g*	*h*	*j*
B_{35}	-	-	-	-	-	-	-	-	71
A_{45}	0	29	38	51	6	45	64	83	-
A	0	15	23	32	5	17	24	36	-
B	0	8	15	27	0	6	12	48	-
E	0	2	4	7	0	0	5	18	-
F	0	0	1	2	0	0	3	8	-

(b)

SH	**Dist. Phal.**				**Prox. Phal.**				**Palm**	**Lat.**
Load	*a*	*b*	*c*	*d*	*e*	*f*	*g*	*h*	*j*	*k*
A_{50}	-	-	-	-	-	-	-	-	86	-
A_{45}	4	7	11	16	17	21	39	75	-	-
A	2	3	6	7	7	13	20	25	-	6
B	1	2	4	4	4	8	14	16	-	4
C	1	2	2	4	4	7	11	14	-	4
D	1	2	3	3	4	7	9	11	-	3

(c)

Case i	**WM**		**SH**	
Iteration	A_{20}	A_{30}	A_{20}	A_{30}
1	86.9	86.5	75.4	78.0
2	87.2	85.4	74.8	77.3
3	87.0	85.8	75.0	77.5
4	86.4	86.7	74.6	77.3
5	86.2	85.7	74.4	77.1
AVG.	**86.7**	**86.0**	**74.8**	**77.4**

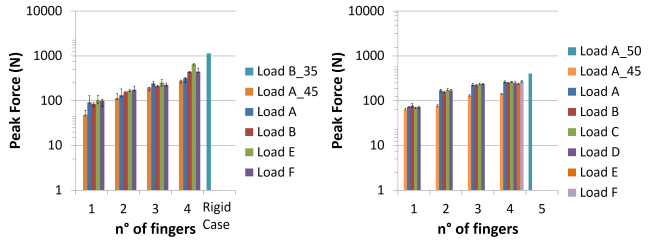

(a) (b)

Fig. 9. Figure shows the peak forces measured during impact test *e-hd*/all load level respectively on a) WM, b) SH. Bars show the median value of each experiment, while the box-plot represents the statistical deviation given by the experimental measurements. For the stiff condition (j) it is reported just the value of the single trial.

load cases and 11 impact condition. We observed that, for under-actuated compliant hand the absorbed energy and the transmitted forces depend on the number of fingers in contact and on the load case. In general, the higher is the absorbed energy, the higher are the transmitted loads. Impacts in the lateral plane are generally less critical then those in the front plane, if joints design allow side bend. Moreover in the tested range, transmitted loads in case (k) are not affected by load level. For the visual representation of the experiment, we opted for pendulum phase diagrams for rendering both the discontinuity in the velocity and the pendulum height variation. Concerning the force measured at the base, we opted for a bar plot with whiskers to show the statistical deviation of the experimental results in a compact way.The main factor causing uncertainty in the measures was under-actuation which does not guarantee a full reproducibility of the hand configuration before the impact. This effect is unavoidable and its entity depends on the mechanical properties of the system. Moreover, at high loads we experienced vibration of the portal structure. Therefore, for executing impacts with higher momentum we consider to increase the portal stiffness, to avoid to affect the pendulum position measurement. Note that, the testing set-up should be constrained to the ground for a correct test execution. The force torque sensor at the base was selected, among the largest sizes commercially available, as trade-off between load capacity and resolution. Despite all, its load range resulted a limiting factor for the set-up and did not allowed to perform impact test on rigid case with high pendulum energy levels, to obtain the ratio of force reduction. Future development consider either to replace it with a larger size, either to sensorize the pendulum tip to measure the force at the impact point to retrieve directly the force transmissibility. Currently, the experimental set-up does not allow to perform impacts along the top plane normal. This case is of interest when the fingers are in a singular configuration. Except for this specific case, impacts along the top plane normal are comparable to the frontal plane case. Comparing the impact tests on WM and SH it is possible to draw several consideration as collateral results of our analysis. Firstly, the presence of the base dampers (structural compliance) lower the energy absorbed and the loads of SH with respect to WM. Secondly, the saturation is more evident in the plot of SH (Fig.7(a)-7(b)), due to the different hand/finger mechanical properties (mass and stiffness). Consequently, SH data have a smaller dispersion due to a higher ratio phalanx mass over ligament stiffness. Lastly, to compare the mechanical robustness of the systems, we performed the most severe impact test (*h-F*) on both the soft-hands. Despite the considerable momentum, the SH, which is made of plastic, was not damaged. Concluding, none of the hands was damaged and the SH performed better both concerning the absorbed energy and the transmitted loads, thanks to lighter fingers and extra compliance at the wrist. We observed that, system robustness of compliant under-actuated hands is provided by design and it is affected by its mass and stiffness properties. Therefore, the use of lightweight material, such as plastic, and distributed compliance is preferable.

VII. CONCLUSIONS

In this work we investigated the problem of robustness of robotic hands for real world applications. We proposed a method, based on Izod impact test, to provide quantitative measures of resilience for robotic hands, and enable the benchmarking of different designs and implementations. We analyzed the dynamic behavior of robotic hands, identifying those parameters that concur to their robustness. Currently, the tests were conducted on two soft robotic hand, we believe the whole community would benefit from widening the discussion, towards a common benchmark.

REFERENCES

[1] O. Khatib, X. Yeh, G. Brantner, B. Soe, B. Kim, S. Ganguly, H. Stuart, S. Wang, M. Cutkosky, A. Edsinger, P. Mullins, M. Barham, C. R. Voolstra, K. N. Salama, M. L'Hour, and V. Creuze, "Ocean one: A robotic avatar for oceanic discovery," *IEEE Robotics Automation Magazine*, vol. 23, no. 4, pp. 20–29, Dec 2016.

[2] F. Negrello, A. Settimi, D. Caporale, G. Lentini, M.Poggiani, D. Kanoulas, L. Muratore, E. Luberto, G. Santaera, L. Ciarleglio, L. Ermini, L. Pallottino, D. Caldwell, N. Tsagarakis, A. Bicchi, M. Garabini, and M. Catalano, "Walk-man humanoid robot: Field experiments in a post-earthquake scenario," *RAM*, 2018.

[3] A. Silwal, J. R. Davidson, M. Karkee, C. Mo, Q. Zhang, and K. Lewis, "Design, integration, and field evaluation of a robotic apple harvester," *Journal of Field Robotics*, vol. 34, no. 6, pp. 1140–1159, 2017.

[4] A. Parmiggiani, L. Fiorio, A. Scalzo, A. V. Sureshbabu, M. Randazzo, M. Maggiali, U. Pattacini, and et al., "The design and validation of the r1 personal humanoid," in *2017 IEEE/RSJ International Conference on Intelligent Robots and Systems (IROS)*, Sept 2017, pp. 674–680.

[5] Ottobock, "Hand prosthesis," accessed on 04 Sept. 2018. [Online]. Available: https://www.ottobock.com/

[6] M. Grebenstein, M. Chalon, G. Hirzinger, and R. Siegwart, "Antagonistically driven finger design for the anthropomorphic dlr hand arm system," in *Humanoid Robots (Humanoids), 2010 10th IEEE-RAS International Conference on*. IEEE, 2010, pp. 609–616.

[7] J. Falco, K. V. Wyk, S. Liu, and S. Carpin, "Grasping the performance: Facilitating replicable performance measures via benchmarking and standardized methodologies," *IEEE Robotics Automation Magazine*, vol. 22, no. 4, pp. 125–136, Dec 2015.

[8] R. Deimel and O. Brock, "A compliant hand based on a novel pneumatic actuator," in *2013 IEEE International Conference on Robotics and Automation*, May 2013, pp. 2047–2053.

[9] Deimel and Brock, *Soft Hands for Reliable Grasping Strategies*. Berlin, Heidelberg: Springer Berlin Heidelberg, 2015, pp. 211–221.

[10] M. Grebenstein, A. Albu-Schäffer, T. Bahls, M. Chalon, O. Eiberger, W. Friedl, R. Gruber, S. Haddadin, U. Hagn, R. Haslinger, H. Höppner, S. Jörg, M. Nickl, A. Nothhelfer, F. Petit, J. Reill, N. Seitz, T. Wimböck, S. Wolf, T. Wüsthoff, and G. Hirzinger, "The dlr hand arm system," in *2011 IEEE International Conference on Robotics and Automation*, May 2011, pp. 3175–3182.

[11] A. M. Dollar and R. D. Howe, "The highly adaptive sdm hand: Design and performance evaluation," *The international journal of robotics research*, vol. 29, no. 5, pp. 585–597, 2010.

[12] M. G. Catalano, G. Grioli, E. Farnioli, A. Serio, C. Piazza, and A. Bicchi, "Adaptive Synergies for the Design and Control of the Pisa/IIT SoftHand," *International Journal of Robotics Research*, vol. 33, pp. 768–782, 2014.

[13] "Super Robust Robot Hand," Jan. 25 2011. [Online]. Available: https://www.youtube.com/watch?v=YqmRKqFqiok

[14] "SDM hand," Mar. 28 2013. [Online]. Available: https://www.youtube.com/watch?v=-JSfZMLhX5g

[15] T. Baumeister, A. M. Sadegh, and E. A. Avallone, "Friction," *Marks' Standard Handbook for Mechanical Engineers, 11th ed., McGraw-Hill, New York*, 2007.

[16] "ISO 148-1 metallic materials — Charpy pendulum impact test — part 1: Test method." 2016.

[17] "ISO 148-2 metallic materials — Charpy pendulum impact test — part 2: Verification of testing machines." 2016.

[18] "ISO 148-3 metallic materials — Charpy pendulum impact test — part 3: Preparation and characterization of charpy v-notch test pieces for indirect verification of pendulum impact machines." 2016.

[19] J. R. Amend, E. Brown, N. Rodenberg, H. M. Jaeger, and H. Lipson, "A positive pressure universal gripper based on the jamming of granular material," *IEEE Transactions on Robotics*, vol. 28, no. 2, pp. 341–350, April 2012.

[20] G. Berselli, A. Guerra, G. Vassura, and A. O. Andrisano, "An engineering method for comparing selectively compliant joints in robotic structures," *IEEE/ASME Transactions on Mechatronics*, vol. 19, no. 6, pp. 1882–1895, Dec 2014.

[21] C. D. Santina, C. Piazza, G. M. Gasparri, M. Bonilla, M. G. Catalano, G. Grioli, M. Garabini, and A. Bicchi, "The quest for natural machine motion: An open platform to fast-prototyping articulated soft robots," *IEEE Robotics Automation Magazine*, vol. 24, no. 1, pp. 48–56, March 2017.